Journal of Applied Physics

A crystalline oxide passivation on $In_{0.53}Ga_{0.47}As$ (100)

Cite as: J. Appl. Phys. **121**, 125302 (2017); https://doi.org/10.1063/1.4979202
Submitted: 14 December 2016 . Accepted: 15 March 2017 . Published Online: 29 March 2017

Xiaoye Qin, Wei-E Wang, Ravi Droopad, Mark S. Rodder, and Robert M. Wallace

A crystalline oxide passivation on $In_{0.53}Ga_{0.47}As$ (100)

Xiaoye Qin,[1,a)] Wei-E Wang,[2] Ravi Droopad,[3] Mark S. Rodder,[2] and Robert M. Wallace[1,b)]
[1]*Department of Materials Science and Engineering, University of Texas at Dallas, Richardson, Texas 75080, USA*
[2]*Advanced Logic Lab, Samsung Semiconductor, Inc., Austin, Texas 78754, USA*
[3]*Ingram School of Engineering, Texas State University, San Marcos, Texas 78666, USA*

(Received 14 December 2016; accepted 15 March 2017; published online 29 March 2017)

The passivation of $In_{0.53}Ga_{0.47}As$ surfaces is highly desired for transistor performance. In this study, the feasibility of a crystalline oxide passivation on $In_{0.53}Ga_{0.47}As$ (100) is demonstrated experimentally. The (3×1) and (3×2) crystalline oxide reconstructions are formed on the de-capped $In_{0.53}Ga_{0.47}As$ (100) surfaces through the control of the surface oxidation states. By monitoring the evolution of chemical states and associated structures of the $In_{0.53}Ga_{0.47}As$ (100) surfaces upon O_2 and subsequent atomic hydrogen exposure, we find that the control of the Ga oxide states is critical to the formation of the crystalline oxide reconstructions. The stability of the crystalline oxide layers upon the atomic layer deposition of HfO_2 is investigated as well. Furthermore, the capacitance voltage behavior of metal oxide semiconductor capacitors with an HfO_2 dielectric layer reveals that the crystalline oxide reconstructions result in a decrease in the density of interface traps (D_{it}) from $\sim 1 \times 10^{13}\,cm^{-2}\,eV^{-1}$ to $\sim 1 \times 10^{12}\,cm^{-2}\,eV^{-1}$ compared with the de-capped surface. The crystalline oxide passivation offers a platform to develop $In_{0.53}Ga_{0.47}As$ devices with a low density of interface states. *Published by AIP Publishing*. [http://dx.doi.org/10.1063/1.4979202]

I. INTRODUCTION

III-Arsenide semiconductors have significant potential as the channel materials for future advanced metal-oxide-semiconductor field effect transistors (MOSFETs).[1,2] Among the III-As family, $In_{0.53}Ga_{0.47}As$ is a leading candidate as a channel material because of its high electron mobility and suitable bandgap. One key issue that is limiting its development is the high density of interface traps (D_{it} and oxide dielectric border traps) between the $In_{0.53}Ga_{0.47}As$ and the amorphous high k dielectric layer, such as disorder-induced gap states.[3–8]

Introducing an ordered interface is expected to decrease the density of the defect states at and near the interface region. Recently, for example, it has been demonstrated that a crystalline oxide reconstruction can reduce the D_{it} effectively on InAs (100).[9–11] Priyantha *et al*. reported monolayer Ga_2O crystalline oxide deposition on GaAs using molecular beam epitaxy.[12] A crystalline oxide with a (3×1) reconstruction is predicted to be possible on InGaAs (100) as well;[13] however, the experimental realization of the crystalline reconstruction has not been reported. This is because manipulating the oxidation of the ternary InGaAs compound is much more challenging than that of InAs due to the different oxidation activities of indium and gallium. The (3×1)-O reconstruction on InAs (100) is produced by exposure to O_2 gas at specific pressures and temperatures.[14] To satisfy the same bonding configuration, systematic experiments are employed for $In_{0.53}Ga_{0.47}As$ (100) in this work. The feasibility of (3×1)-O reconstruction on $In_{0.53}Ga_{0.47}As$ (100) is demonstrated. Moreover, another distinctive (3×2)-O reconstruction, through tailoring the oxidized $In_{0.53}Ga_{0.47}As$ (100) surface using an atomic hydrogen (AH) exposure, is reported in this work. The capacitance voltage behavior of metal oxide semiconductor capacitors with an HfO_2 dielectric layer reveals that these two types of oxygen reconstructions offer a passivation scheme for $In_{0.53}Ga_{0.47}As$ (100) surfaces, reducing the density of the interface traps with subsequent atomic layer deposition (ALD) of high-k oxides.

II. EXPERIMENTAL DETAILS

$In_{0.53}Ga_{0.47}As$ samples with a $\sim$50 nm thick As_2 cap layer were grown via molecular beam epitaxy on heavily doped n-type InP (100) wafers with a carrier concentration of $10^{18}\,cm^{-3}$, purchased from Wafer Technology Ltd. The As_2 capping layer prevented the oxidation of the underlying $In_{0.53}Ga_{0.47}As$ surfaces when these wafers were exposed to air after growth. A $\sim$1 cm $\times$ 1 cm sample cleaved from the As_2-capped wafers was mounted at the center of a circular Mo plate and then loaded into an ultra-high vacuum (UHV) system described elsewhere.[15] To ensure the consistency among the experiments, all $In_{0.53}Ga_{0.47}As$ samples described in this work were loaded on the same Mo plate. In order to remove the As_2 cap layer, these samples were radiatively heated at 350 °C for 1 h under UHV conditions to get a (4×2) surface reconstruction with no evidence of carbon or oxygen confirmed by x-ray photoelectron spectroscopy (XPS) and low energy electron diffraction (LEED) in the analysis chamber, where the base pressure was maintained at $P_{base} = 3 \times 10^{-9}$ mbar. As Kummel *et al*. reported, this de-capping method could contribute to a flat $In_{0.53}Ga_{0.47}As$ surface with a root mean square (rms) roughness of $\sim$0.1 nm.[16–19] All O_2 and atomic hydrogen (AH) exposure experiments were carried out in a process chamber with the

a)Electronic mail: xxq102020@utdallas.edu
b)Electronic mail: rmwallace@utdallas.edu

bass pressure of 1×10^{-9} mbar. After every treatment in the UHV process chamber, samples were transferred through a UHV transfer tube ($P_{base} = 3 \times 10^{-11}$ mbar) to an analysis chamber, in which XPS and LEED were carried out. In O_2 exposure treatments, the partial pressure of high purity O_2 gas (99.999%) was adjusted to be in the range from 1×10^{-7} to 1×10^{-3} mbar through a precision leak value. The AH was generated using a hydrogen gas thermal cracking source consisting of a fine capillary tube, through which high purity H_2 (99.9999%) was admitted, surrounded by a tungsten filament heated to ~1400 °C by direct current heating (HABS-40, MBE Kommponenten, Germany). The total background pressure of H_2 in the chamber during the exposure could be adjusted among 1×10^{-7} to 1×10^{-5} mbar. The substrate temperature can be set from room temperature to 700 °C.

A commercial ALD system (Picosun PR-200 PEALD reactor (Masala, Finland)) integrated to the system by a buffer chamber and the transfer tube was employed to grow the HfO_2 film. The ALD system can operate under thermal and plasma enhanced modes. In this work, the thermal ALD mode was employed, and one full thermal ALD HfO_2 sequence was 0.1s tetrakis (dimethylamino) hafnium (TDMA-Hf) + 10 s Ar purge + 0.1 s deionized H_2O + 10 s Ar purge. The substrate in the ALD reactor could be heated from room temperature to 550 °C. The TDMA-Hf precursor (SIGMA-ALDRICH) temperature was set at 85 °C, and the water was kept at room temperature. High purity (99.9999%) Ar was used as the precursor carrier and purging gas. The base pressure and working pressure of the reactor were 0.01 and 5 mbar, respectively.

XPS and LEED located in the interconnected analysis chamber were utilized to establish the chemical states and structures of surfaces, respectively, where the pressure was maintained at 7×10^{-10} mbar. Monochromatic XPS using Al Kα ($h\nu = 1486.7$ eV) with a 7 channel analyzer, using a pass energy of 15 eV for all scans taken of the In $3d_{5/2}$, Ga $2p_{3/2}$, As $2p_{3/2}$, Hf 4*f*, O 1*s*, and C 1*s* core level regions were collected. These regions were carefully chosen as they exhibit the most sensitivity as well as the best signal/noise ratio for the spectral peaks of the corresponding elements. Because the Hf 4*f* core level overlaps with the In 4*d* core level, the alternative Hf 4*d* core level spectra were recorded as well, and used in tracking the growth of HfO_2. XPS peak deconvolution was carried out using an AAnalyzer software with a detailed peak fitting procedure described elsewhere.[20] In order to provide a consistent fit for the core level peaks, reference spectra were acquired from the de-capped InGaAs sample with no evidence of carbon or oxygen present within the detection limits. Using the spectra from this sample, Gaussian and Lorentzian bulk peak parameters were determined for the In $3d_{5/2}$, Ga $2p_{3/2}$, and As $2p_{3/2}$ peaks which were fixed in all subsequent peak fits. LEED patterns were acquired at an energy of 60 eV.

The metal oxide semiconductor capacitors were also fabricated for capacitance–voltage (C-V) measurements. First, de-capped and crystalline oxide $In_{0.53}G_{0.47}As$ samples were prepared in the process chamber and verified by XPS and LEED, followed by 50 cycles of ALD HfO_2 grown at 120 °C, which was thick enough to avoid spurious interface oxidation in air.[21] Then, these samples were taken out from the system for *ex-situ* metal depositions and post annealing in the clean room facility. The e-beam evaporated Ni gate metal was 80 nm thick with different diameter (50, 100, 200, 300, and 500 μm) circular electrodes using a shadow mask. The back side contact consisted of a blanket e-beam evaporated Ti (20 nm) followed by Au (80 nm). All samples were exposed to a 1 min 350 °C forming gas anneal (FGA, 5% H_2, and 95% N_2) after the metal depositions. C-V curves were measured (1 kHz to 1 MHz) using an Agilent 4284 LCR meter at a step of 0.01 V in the dark at room temperature. At least five C-V measurements were performed on different gates on each capacitor sample to examine the uniformity across the capacitors.

III. RESULTS AND DISCUSSION

A. (3 × 1)-O reconstruction on $In_{0.53}Ga_{0.47}As$ (100)

In our previous study, the (3 × 1)-O reconstruction on InAs (100) was obtained by exposing the de-capped InAs with an initial (4 × 2) reconstruction to O_2 gas ($3 \pm 0.1 \times 10^{-6}$ mbar) in a temperature range of 290–330 °C for 20 min.[14] The *in situ* XPS of that InAs surface reveals the coexistence of In_2O (In^{1+}) and As_2O_3 (As^{3+}) in the (3 × 1)-O layer. At the onset of this study, we have repeated the same process recipe on the $In_{0.53}Ga_{0.47}As$ (100) surface using the same experimental tools; however, no ordered LEED pattern is detected from this treatment (see Fig. 1(a)). The corresponding XPS spectra are shown in Figs. 2(a)–2(e). Compared with the surface chemical states detected on the (3 × 1)-O reconstructed surface of InAs (100), the In^{1+}/Ga^{1+} state is detected whereas the As^{3+} state is absent (prior *in situ* XPS studies of carefully controlled Ga_2O deposition on the de-capped $In_{0.53}Ga_{0.47}As$ surface have built a good XPS reference and enabled the deconvolution of the Ga^{1+} and In^{1+} oxidation states with high confidence.[22–24]). If the integration of In^{1+}/Ga^{1+} and As^{3+} states is the necessary condition of the (3 × 1)-O reconstruction on the $In_{0.53}Ga_{0.47}As$ (100), the absence of the As^{3+} state should be responsible for the failure of the reconstruction formation. Another noticeable difference is the appearance of the Ga^{3+} state that is another possible reason to destroy the ordered structure. As a result of the growth of the native oxides, a small peak attributed to As dimer (As^0) formation is detected, leaving the interface locally arsenic-rich.[25–27] In contrast, a longer O_2 gas exposure time at the same temperature triggers the formation of the As^{3+} chemical state; however, there is still no ordered LEED pattern from an ordered surface oxide reconstruction detected (see Fig. 1(b) where only a faint (1 × 1) pattern is detected and associated with the underlying substrate). It is noted that an ordered oxide layer is not obtained even with a dramatic increase in In/Ga oxide

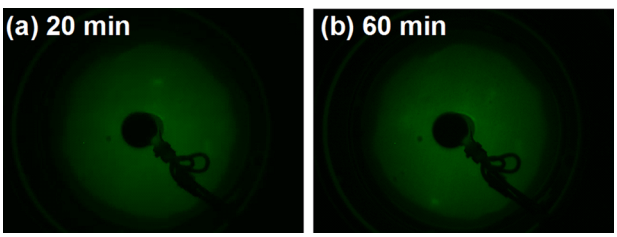

FIG. 1. LEED images after exposing the de-capped $In_{0.53}Ga_{0.47}As$ samples to 3×10^{-6} mbar O_2 gas at 310 °C for (a) 20 and (b) 60 min.

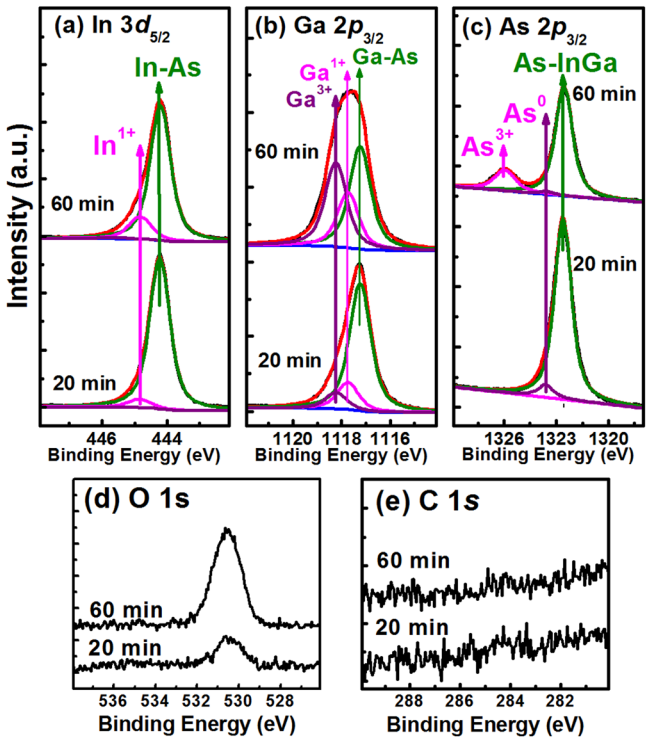

FIG. 2. XPS spectra of (a) In $3d_{5/2}$, (b) Ga $2p_{3/2}$, (c) As $2p_{3/2}$, (d) O 1*s*, and (e) C 1*s* after exposing the de-capped $In_{0.53}Ga_{0.47}As$ samples to 3×10^{-6} mbar O_2 gas at 310 °C for 20 and 60 min.

formation, especially the Ga^{3+} chemical state (Figs. 2(a) and 2(b)). This amorphous oxide formation is consistent with the increase of the O 1*s* peak intensity (Fig. 2(d)).

Interestingly, the As^0 dimer chemical state decreases in intensity with increasing In/Ga oxide concentration for the 60 min O_2 exposure, in contrast to the intensity of the As^0 state after the 20 min O_2 exposure as an accompaniment of the In/Ga oxides. This is due to the prolonged O_2 exposure time and the resultant conversion of the As dimer to the As^{3+} state, and is confirmed by the higher intensity ratio (25%) of the As^{3+} to As-InGa (substrate) on $In_{0.53}Ga_{0.47}As$ compared with that detected (~20%) on InAs,[9] based upon the ratios extracted from the As $2p_{3/2}$ region. It has been demonstrated that the In^{3+} state on InAs contributes to the amorphous interface;[14] therefore, the high intensity of the Ga^{3+} state likely plays the same role in disordering the surface and inhibiting the occurrence of the (3×1)-O reconstruction. In summary, avoiding the Ga^{3+} state and keeping the As^{3+} state must be considered simultaneously in regard to the formation of an ordered oxide interface.

Through optimizing parameters in a wide range of substrate temperature (250–400 °C), O_2 pressure (10^{-7}–10^{-3} mbar), and O_2 exposure time (1–60 min), a sharp (4×2) reconstruction of de-capped $In_{0.53}Ga_{0.47}As$ was successfully converted to a (3×1)-O reconstruction, after exposure to 5×10^{-5} mbar O_2 gas at 350 °C for 5 min (see Fig. 3). The deconvoluted In $3d_{5/2}$, Ga $2p_{3/2}$, and As $2p_{3/2}$ spectra are shown in Figs. 4(a)–4(c). The In^{1+}/Ga^{1+} and As^{3+} oxidation states are detected on this ordered surface with a low concentration of the Ga^{3+} state, consistent with the assumption above on the chemical states required for the ordered oxide

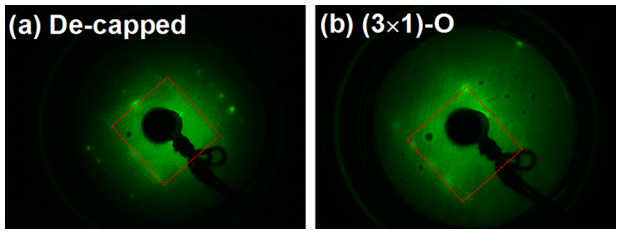

FIG. 3. LEED images from (a) the de-capped $In_{0.53}Ga_{0.47}As$ surface and (b) after exposure to 1×10^{-5} mbar O_2 gas at 350 °C for 5 min.

reconstruction on this surface. The low concentration of the As^0 state (see Fig. 4(c)) is a promising sign, indicative of a reduction of D_{it}, since the As^0 state is well known as a source of gap states at InGaAs surface.[3,25]

It is thus reasonable to assume that the (3×1)-O on $In_{0.53}Ga_{0.47}As$ has the same reconstruction and bonding configuration as that detected on InAs. It should be noted that, even though this set of parameters has been optimized through numerous experiments, the LEED pattern diffraction spots are less sharp than that observed on the (3×1)-O on InAs, because of the rapid appearance of the persistent Ga^{3+} state at the surface. The formation of this oxidation state apparently disrupts the ordered (3×1) surface periodicity. Regardless, this result establishes the pathway towards the formation of a (3×1)-O crystalline oxide on $In_{0.53}Ga_{0.47}As$.

B. An alternative (3×2)-O reconstruction on $In_{0.53}Ga_{0.47}As$ (100)

As discussed in the section on the formation of the (3×1)-O reconstruction on $In_{0.53}Ga_{0.47}As$, it is difficult to avoid the generation of the Ga^{3+} state by manipulating the conditions of the O_2 gas exposures (temperature, time, and pressure). Ide and Yamada previously reported that an AH exposure could attack the Ga^{3+} state prior to the Ga^{1+} state on GaAs, and the remnant of the Ga^{1+} state can survive

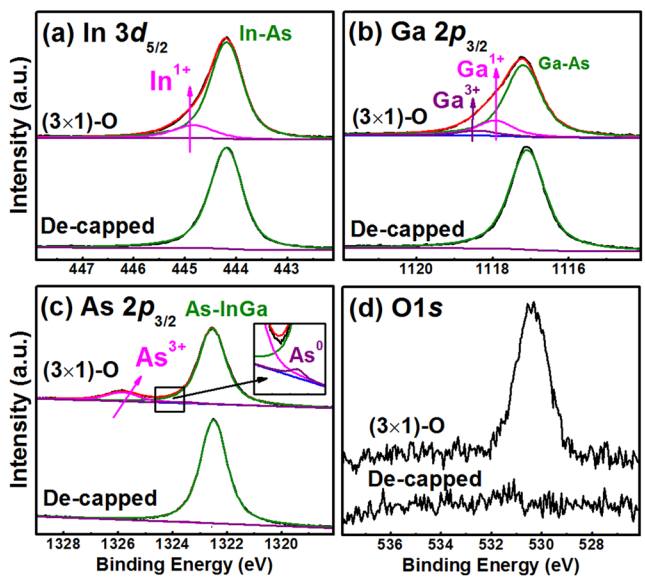

FIG. 4. XPS spectra of (a) In $3d_{5/2}$, (b) Ga $2p_{3/2}$, (c) As $2p_{3/2}$, and (d) O 1*s* from the de-capped $In_{0.53}Ga_{0.47}As$ surface and after exposure to 1×10^{-5} mbar O_2 gas at 350 °C for 5 min.

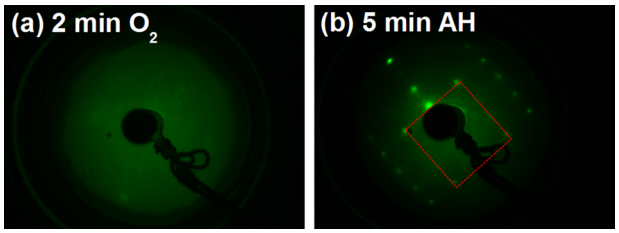

FIG. 5. LEED images after exposure to 1×10^{-4} mbar O_2 for (a) 2 min at 320 °C and (b) 1×10^{-6} mbar AH at 350 °C for 5 min.

during the AH exposure in a suitable temperature range.[28] This behavior suggests that the Ga^{3+} state may be controlled by exposing the oxidized $In_{0.53}Ga_{0.47}As$ to AH. Although oxide states such as In^{1+} and As^{3+} states might also be reduced or even removed after the AH exposure,[29] this "reversible" oxide decomposition process opens another window to observing the properties of these ordered oxides.

The oxidized sample surface was prepared through exposing the de-capped $In_{0.53}Ga_{0.47}As$ to 1×10^{-4} mbar O_2 gas at 320 °C for 2 min, resulting in an amorphous surface (see Fig. 5(a)). The In^{1+}, Ga^{1+}, Ga^{3+}, and As^{3+} states are all detected (see Figs. 6(a)–6(c)). Interestingly, the surface presents a distinctive and sharp (3×2) reconstruction after the 5 min AH exposure (1×10^{-6} mbar) at 350 °C (see Fig. 5(b)). In terms of the XPS from this ordered surface, the In-oxides, Ga^{3+}, As^{3+}, and As^0 are all below the XPS detection limits, while the Ga^{1+} state survives. Similar to the behavior reported on GaAs, the atomic hydrogen exposure reduces the Ga^{3+} state below the limit of detection, and leaving the Ga^{1+} state.[28] Consequently, the remnant of the Ga^{1+} state detected consists of the (3×2)-O reconstruction on $In_{0.53}Ga_{0.47}As$. Although the reconstructions of III-As have been studied for decades,[13,17,18,30,31] the (3×2)-O reconstruction has not yet been reported. In particular, Hale *et al*. reported a monolayer of Ga_2O with a (2×2) surface structure on $c(2 \times 8)/(2 \times 4)$ GaAs (As terminated), by evaporating pure Ga_2O_3 from an effusion cell.[31] The Ga_2O inserts into As-As bonds to restore the surface to bulk-like termination.[31] However, this configuration could not be repeated on the (4×2) $In_{0.53}Ga_{0.47}As$ surface (terminated by In/Ga), where the Ga_2O (Ga^{1+}) forms disordered structures with the large flat terraces.[17] The structural model of the (3×2)-O reconstruction is still uncertain; however, it should be closely related to the stoichiometry of In/Ga since the (3×2)-O reconstruction has not been found on InAs (100) or GaAs (100). The (3×2)-O reconstruction may be a specific type of reconstruction on $In_{0.53}Ga_{0.47}As$ (100) with the single Ga_2O state. Additionally, the reason for exposing the sample to 1×10^{-4} mbar O_2 is driven here by the desire to obtain a suitable Ga^{3+} state concentration, which is critical for the subsequent formation of the (3×2)-O reconstruction. A higher concentration of Ga^{3+} state will result in the complete amorphous oxide at and near the surface while a lower Ga^{3+} state could not prevent the rapid decomposition of the Ga^{1+} state after the atomic hydrogen exposure. Apparently, either a lower or higher concentration of the Ga^{3+} state makes the reconstruction formation process more difficult, and perhaps practically impossible.

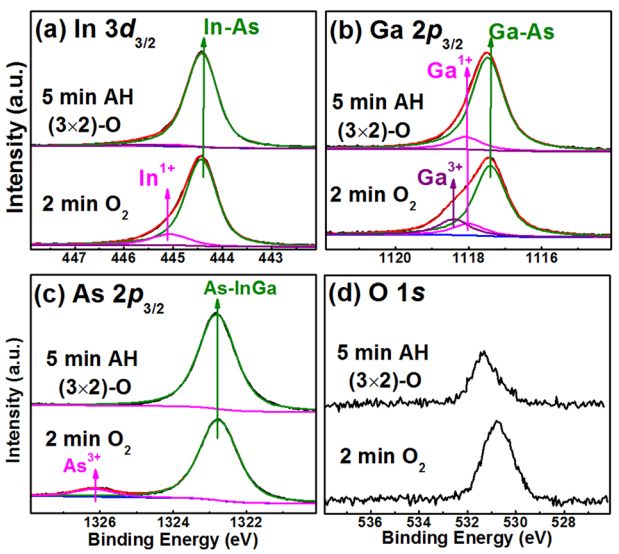

FIG. 6. XPS spectra of (a) In $3d_{5/2}$, (b) Ga $2p_{3/2}$, (c) As $2p_{3/2}$, and (d) O 1*s* after exposure to 1×10^{-4} mbar O_2 for 2 min at 320 °C and 1×10^{-6} mbar AH at 350 °C for 5 min.

C. ALD of HfO_2 on de-capped $In_{0.53}Ga_{0.47}As$

Many studies have been done to reduce native oxides as low as possible prior to subsequent atomic layer deposition (ALD) of high-k dielectrics, as native oxides, especially the Ga^{3+} state, are considered as a potential source of defects.[27,32–36] However, a clean surface could not ensure the absence of native oxides due to the regrowth after exposure to ALD of oxides. The de-capped $In_{0.53}Ga_{0.47}As$ samples with the carbon and oxygen free surfaces (see Figs. 7(b) and 7(c)) were

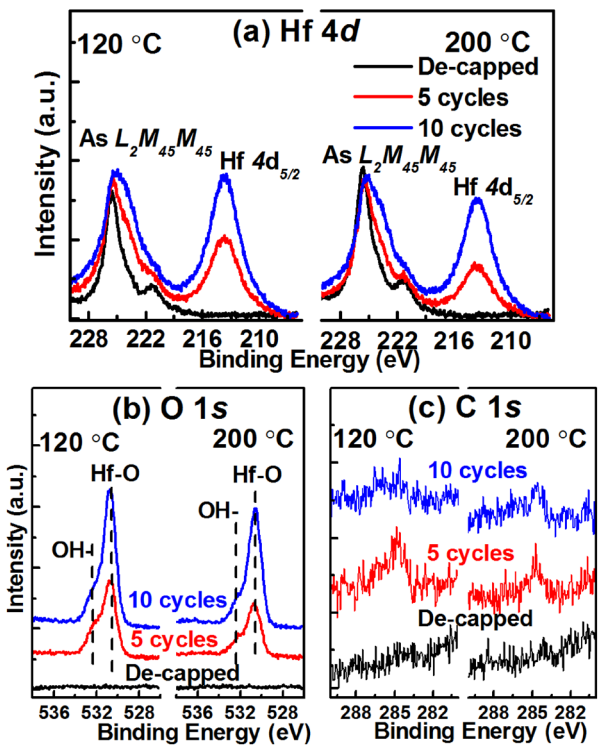

FIG. 7. XPS spectra of (a) Hf 4*d*, (b) O 1*s*, and (c) C 1*s* from the de-capped $In_{0.53}Ga_{0.47}As$ surface, after 5 cycles, and after 10 cycles of HfO_2 grown at 120 and 200 °C.

prepared to investigate the interaction with subsequent ALD of HfO_2. Two substrate temperatures during deposition, 120 and 200 °C, were used. The Hf 4*d*, O 1*s*, and C 1*s* core levels (see Figs. 7(a)–7(c)) from the de-capped surface, after 5 cycles of HfO_2, and after a total of 10 cycles of HfO_2 exhibit the growth and quality (low carbon and OH- residues) of the HfO_2 film. The appearance and increase of the Hf 4*d* peak after 5 and 10 cycles of HfO_2, respectively, indicate that the growth of HfO_2 is detected. Regarding the O 1*s* and C 1*s* peak intensity levels, the Hf-O is detected accompanying some -OH bond incorporation into the film consistent with our previous work,[37] and the carbon concentration is near the XPS detection limit. Overall, the reaction between the TDMA-Hf and H_2O appears to be complete.

Moreover, there are some detectable In and Ga oxidation states (see Figs. 8(a) and 8(c)), suggesting the detection of oxidation at the de-capped $In_{0.53}Ga_{0.47}As$ surface after 5 cycles of HfO_2. The additional 5 cycles of HfO_2 (corresponding to a total exposure of 10 cycles) contributes to an increase of oxide formation, as detected by the In^{1+} state. If more than 15 cycles of HfO_2 are deposited, an accurate fitting of the XPS spectra is challenging because of the low signal-to-noise ratio of attenuated substrate peaks. The ratios of the In and Ga oxide states to substrate signals are plotted in Figs. 8(b) and 8(d), showing the evolution of the oxidation after exposure to ALD of HfO_2. The As^0 state forms as a result of the growth of native oxides on the $In_{0.53}Ga_{0.47}As$. Thus, a carbon and oxide free $In_{0.53}Ga_{0.47}As$ surface cannot avoid the regrowth of the interfacial oxide layer with As dimer formation (see Figs. 8(e) and 8(f)). Considering that the low pressure (1×10^{-6}–1×10^{-4} mbar) of the O_2 exposure can contribute to the rapid oxidation of the de-capped $In_{0.53}Ga_{0.47}As$ surface, this conclusion is not a surprise. In ALD, the H_2O vapor pressure at room temperature is ~28 mbar and the base pressure is 10^{-2} mbar; both are much higher than the O_2 pressure in the resultant O_2 exposure experiments above.

D. ALD of HfO_2 on (3 × 1)-O and (3 × 2)-O $In_{0.53}Ga_{0.47}As$

The interfaces between ALD HfO_2 and $In_{0.53}Ga_{0.47}As$ with (3 × 1)-O and (3 × 2)-O reconstructions are investigated using *in situ* XPS. According to our previous work, the As^{3+} state in (3 × 1)-O layer on InAs can survive only at a relatively low temperature because the TDMA-Hf precursor could reduce and even remove the As^{3+} state quickly at high temperature.[14] This phenomenon, the so-called "clean up" effect, has already been reported and discussed in various III–V semiconductors (InAs,[27] InGaAs,[27] InP,[38] GaP,[39] etc.). A substrate temperature of 120 °C was chosen during the deposition, without reactions with the As^{3+} state at the (3 × 1)-O layer, as Fig. 9(c) shows. After 5 cycles of HfO_2,

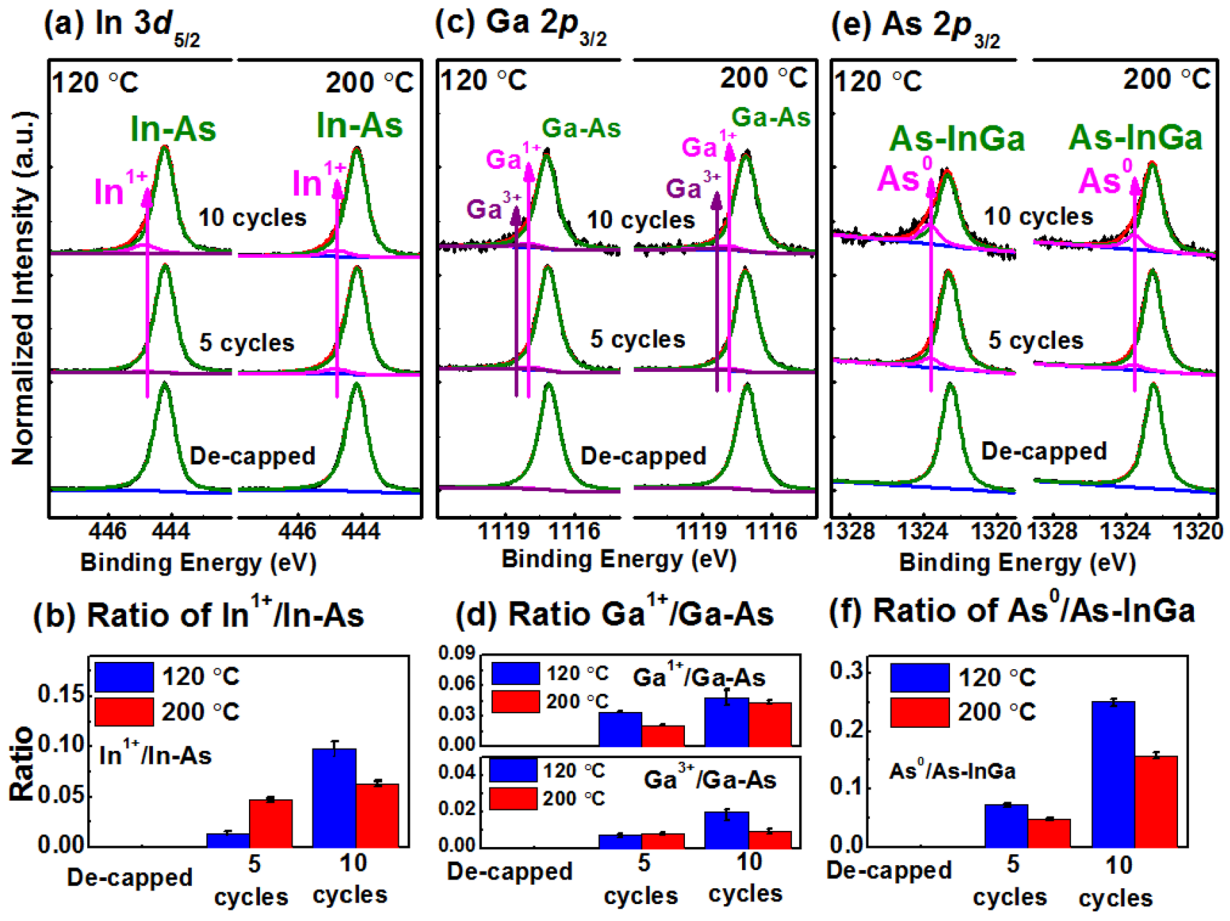

FIG. 8. XPS spectra of (a) In $3d_{5/2}$, (c) Ga $2p_{3/2}$, and (e) As $2p_{3/2}$ from the de-capped $In_{0.53}Ga_{0.47}As$ surface, after 5 cycles, and after 10 cycles of HfO_2 grown at 120 and 200 °C. Ratios of (b) In^{1+} to In-As, (d) Ga^{1+}/Ga^{3+} to Ga-As, and (f) As^0 to As-InGa are shown as well.

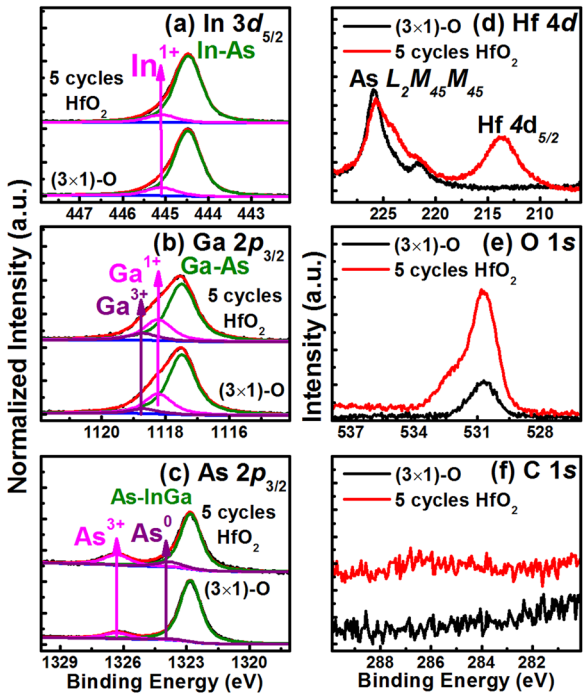

FIG. 9. XPS spectra of (a) In $3d_{5/2}$, (b) Ga $2p_{3/2}$, (c) As $2p_{3/2}$, (d) Hf 4*d*, (e) O 1*s*, and (f) C 1*s* before and after 5 cycles of HfO_2 on (3 × 1)-O $In_{0.53}Ga_{0.47}As$.

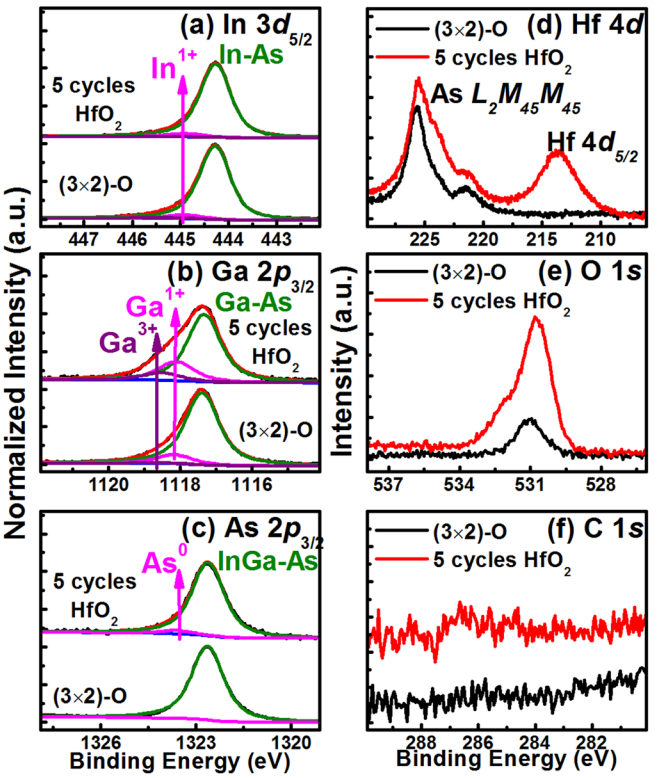

FIG. 10. XPS spectra of (a) In $3d_{5/2}$, (b) Ga $2p_{3/2}$, (c) As $2p_{3/2}$, (d) Hf 4*d*, (e) O 1*s*, and (f) C 1*s* before and after 5 cycles of HfO_2 on (3 × 2)-O $In_{0.53}Ga_{0.47}As$.

the In^{1+} and Ga^{1+} states remain unchanged while the unsaturated Ga^{3+} state increases slightly (see Figs. 9(a) and 9(b)).

The ALD HfO_2 oxidizes the gallium at the (3 × 2)-O reconstructed surface as well, with evidence of increasing the Ga^{1+} state and the detection of the Ga^{3+} state in Fig. 10(b). The As^0 dimer state also appears as a result of the formation of oxides (see Figs. 9(c) and 10(c)).[14,27] Overall, these changes are similar to the interaction between the de-capped surfaces and ALD HfO_2. Instead of the "clean-up" effect, the oxidation reaction with the water precursor changes the surface slightly. As indicators of HfO_2 growth, the presence of Hf $4d_{5/2}$ (see Figs. 9(d) and 10(d)) and the increase of the O 1*s* peak intensity (see Figs. 9(e) and 10(e)) reflect the normal growth of HfO_2 with a low concentration of carbon contamination (see Figs. 9(f) and 10(f)). It is also noted that the ALD process employed here for HfO_2 on the ordered interfacial oxide layer formed on $In_{0.53}Ga_{0.47}As$ is significantly different than that observed for Al_2O_3 formation, where a more aggressive chemical reaction takes place resulting in the removal of the crystalline oxides.[24,40] The thicknesses of 5 cycles of HfO_2 film at 120 °C on de-capped, (3 × 1)-O, or (3 × 2)-O $In_{0.53}Ga_{0.47}As$ is ∼0.5 ± 0.1 nm based on the attenuation of Ga $2p_{3/2}$. There is no obvious nucleation difference on these three substrates, which is likely due to the low nucleation temperature and the weak reaction between the precursors and the substrates.

E. Capacitance–voltage characterization

Multiple frequency C-V curves from 50 cycles of HfO_2 on de-capped, (3 × 1)-O, and (3 × 2)-O $In_{0.53}Ga_{0.47}As$ capacitors are plotted in Fig. 11. The thicknesses of the HfO_2 films are ∼5 nm verified by *ex situ* ellipsometry. Multi-frequency C-V measurement is an effective characterization method to determine the trap density at the oxide/$In_{0.53}Ga_{0.47}As$ interface.[8] As Fig. 11 shows, the capacitance dispersion with the frequency is observed. As the gate bias is swept toward the negative applied voltage, a bump is observed as a result of charges being injected into electronic trap states at the interface. Thus, the magnitude of the bump can be interpreted to obtain a qualitative description of the interface state density (D_{it}). When the C-V modeling is used, the bump can contribute to the quantification of D_{it}.

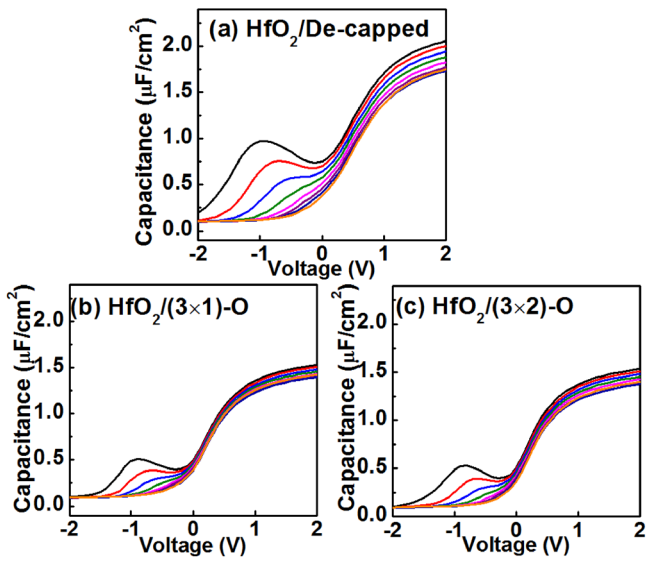

FIG. 11. C-V curves for (a) HfO_2/De-capped $In_{0.53}Ga_{0.47}As$, (b) HfO_2/(3 × 1)-O $In_{0.53}Ga_{0.47}As$, and (c) HfO_2/(3 × 2)-O $In_{0.53}Ga_{0.47}As$ MOSCAPs from 1 kHz to 1 MHz measured at room temperature.

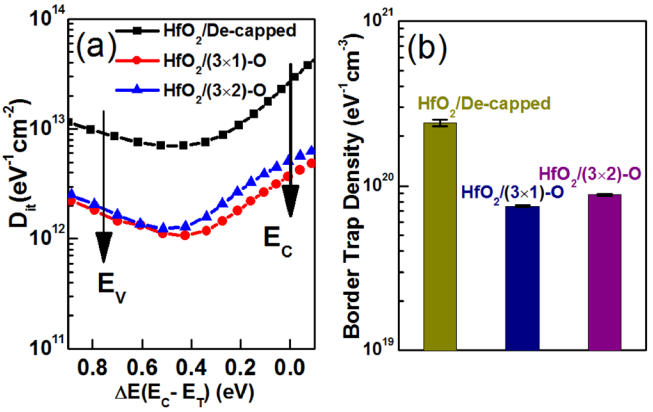

FIG. 12. Extracted (a) D_{it} and (b) border trap densities from the C-V curves in Fig. 11.

The extracted D_{it} is shown in Fig. 12(a) using a high-low frequency method.[41] Compared with the de-capped $In_{0.53}Ga_{0.47}As$, either ordered (3×1)-O or (3×2)-O interfaces reduce the defect response significantly. Fig. 12(b) shows the "border traps" extracted from the C-V dispersion located in the accumulation region according to the method described by Yuan *et al.*[42] Notably, the crystalline (3×1)-O and (3×2)-O reconstructions reduce the density of the response attributed to such border traps as well. Compared with recent work of HfO_2/InGaAs where the D_{it} is in the range of $2\text{–}4 \times 10^{12}\,cm^{-2}\,eV^{-1}$,[33,43,44] the extracted $D_{it} \cong 1 \times 10^{12}\,cm^{-2}\,eV^{-1}$ and the density of border traps ($\sim 7.7 \times 10^{19}\,cm^{-3}\,eV^{-1}$) indicate that a substantial defect passivation is obtained at ALD $HfO_2/In_{0.53}Ga_{0.47}As$ interface. Although different extraction techniques are used in the literature,[33,43,44] the direct comparison of the degree of the dispersion suppression in the C-V curves still shows an obvious enhancement, as a result of the formation of crystalline oxide interfaces which prevent the appearance of As^0 and reduce the dangling bonds. Thus, the incorporation of a crystalline layer is effective to improve the poor interface quality with ALD HfO_2.

IV. CONCLUSION

The (3×1)-O crystalline oxide is formed on the de-capped $In_{0.53}Ga_{0.47}As$ (100) by exposure to O_2 gas with a narrow process window due to the complexity of oxide formation kinetics. Notably, a distinctive (3×2)-O reconstruction is also achieved on the de-capped $In_{0.53}Ga_{0.47}As$ (100) using an optimized two-step of O_2 followed by an atomic hydrogen exposure, which was not previously predicted. The (3×1)-O exhibits the same bonding configuration as the (3×1)-O on InAs with the integration of In^{1+}/Ga^{1+} and As^{3+} chemical states, while the Ga^{1+} state results in the (3×2)-O reconstruction solely. These two types of crystalline oxide interfacial layers show a significant passivation effect resulting in a low D_{it} and border trap density at the interface with the ALD HfO_2. Such crystalline oxide formation could be a useful platform to develop InGaAs semiconductor field effect devices.

[1]A. M. Ionescu and H. Riel, Nature **479**, 329 (2011).
[2]J. A. del Alamo, Nature **479**, 317 (2011).
[3]R. V. Galatage, D. M. Zhernokletov, H. Dong, B. Brennan, C. L. Hinkle, R. M. Wallace, and E. M. Vogel, J. Appl. Phys. **116**, 014504 (2014).
[4]E. J. Kim, L. Wang, P. M. Asbeck, K. C. Saraswat, and P. C. McIntyre, Appl. Phys. Lett. **96**, 012906 (2010).
[5]J. Ahn, T. Kent, E. Chagarov, K. Tang, A. C. Kummel, and P. C. McIntyre, Appl. Phys. Lett. **103**, 071602 (2013).
[6]C. Dou, D. Lin, A. Vais, T. Ivanov, H. P. Chen, K. Martens, K. Kakushima, H. Iwai, Y. Taur, A. Thean, and G. Groeseneken, Microelectron. Reliab. **54**, 746 (2014).
[7]S. Johansson, M. Berg, K.-M. Persson, and E. Lind, IEEE Trans. Electron Devices **60**, 776 (2013).
[8]G. Brammertz, A. Alian, D. H. C. Lin, M. Meuris, M. Caymax, and W.-E. Wang, IEEE Trans. Electron Devices **58**, 3890 (2011).
[9]M. Tuominen, J. Lång, J. Dahl, M. Kuzmin, M. Yasir, J. Mäkelä, J. R. Osiecki, K. Schulte, M. P. J. Punkkinen, P. Laukkanen, and K. Kokko, Appl. Phys. Lett. **106**, 011606 (2015).
[10]M. Passlack, S. W. Wang, G. Doornbos, C. H. Wang, R. Contreras-Guerrero, M. Edirisooriya, J. Rojas-Ramirez, C. H. Hsieh, R. Droopad, and C. H. Diaz, Appl. Phys. Lett. **104**, 223501 (2014).
[11]C. H. Wang, S. W. Wang, G. Doornbos, G. Astromskas, K. Bhuwalka, R. Contreras-Guerrero, M. Edirisooriya, J. S. Rojas-Ramirez, G. Vellianitis, R. Oxland, M. C. Holland, C. H. Hsieh, P. Ramvall, E. Lind, W. C. Hsu, L.-E. Wernersson, R. Droopad, M. Passlack, and C. H. Diaz, Appl. Phys. Lett. **103**, 143510 (2013).
[12]W. Priyantha, G. Radhakrishnan, R. Droopad, and M. Passlack, J. Cryst. Growth **323**, 103 (2011).
[13]M. P. J. Punkkinen, P. Laukkanen, J. Lång, M. Kuzmin, M. Tuominen, V. Tuominen, J. Dahl, M. Pessa, M. Guina, K. Kokko, J. Sadowski, B. Johansson, I. J. Väyrynen, and L. Vitos, Phys. Rev. B **83**, 195329 (2011).
[14]X. Qin, W.-E. Wang, M. S. Rodder, and R. M. Wallace, Appl. Phys. Lett. **109**, 041601 (2016).
[15]R. M. Wallace, ECS Trans. **16**, 255 (2008).
[16]W. Melitz, T. Kent, A. C. Kummel, R. Droopad, M. Holland, and I. Thayne, J. Chem. Phys. **136**, 154706 (2012).
[17]J. Shen, D. L. Feldwinn, W. Melitz, R. Droopad, and A. C. Kummel, Microelectron. Eng. **88**, 377 (2011).
[18]J. Shen, E. A. Chagarov, D. L. Feldwinn, W. Melitz, N. M. Santagata, A. C. Kummel, R. Droopad, and M. Passlack, J. Chem. Phys. **133**, 164704 (2010).
[19]D. L. Feldwinn, J. B. Clemens, J. Shen, S. R. Bishop, T. J. Grassman, A. C. Kummel, R. Droopad, and M. Passlack, Surf. Sci. **603**, 3321 (2009).
[20]A. Herrera-Gómez, A. Hegedus, and P. L. Meissner, Appl. Phys. Lett. **81**, 1014 (2002).
[21]S. McDonnell, H. Dong, J. M. Hawkins, B. Brennan, M. Milojevic, F. S. Aguirre-Tostado, D. M. Zhernokletov, C. L. Hinkle, J. Kim, and R. M. Wallace, Appl. Phys. Lett. **100**, 141606 (2012).
[22]C. L. Hinkle, M. Milojevic, E. M. Vogel, and R. M. Wallace, Appl. Phys. Lett. **95**, 151905 (2009).
[23]J. Mäkelä, M. Tuominen, M. Kuzmin, M. Yasir, J. Lång, M. P. J. Punkkinen, P. Laukkanen, K. Kokko, K. Schulte, J. Osiecki, and R. M. Wallace, Appl. Surf. Sci. **329**, 371 (2015).
[24]M. Milojevic, R. Contreras-Guerrero, E. O'Connor, B. Brennan, P. K. Hurley, J. Kim, C. L. Hinkle, and R. M. Wallace, Appl. Phys. Lett. **99**, 042904 (2011).
[25]J. Robertson, Y. Guo, and L. Lin, J. Appl. Phys. **117**, 112806 (2015).
[26]J. Robertson, Appl. Phys. Lett. **94**, 152104 (2009).
[27]B. Brennan, D. M. Zhernokletov, H. Dong, C. L. Hinkle, J. Kim, and R. M. Wallace, Appl. Phys. Lett. **100**, 151603 (2012).
[28]Y. Ide and M. Yamada, J. Vac. Sci. Technol. A **12**, 1858 (1994).
[29]B. Brennan, K. Kumarappan, and G. Hughes, Phys. Status Solidi RRL **7**, 989 (2013).
[30]J. B. Clemens, S. R. Bishop, D. L. Feldwinn, R. Droopad, and A. C. Kummel, Surf. Sci. **603**, 2230 (2009).
[31]M. J. Hale, S. I. Yi, J. Z. Sexton, A. C. Kummel, and M. Passlack, J. Chem. Phys. **119**, 6719 (2003).
[32]C. L. Hinkle, E. M. Vogel, P. D. Ye, and R. M. Wallace, Curr. Opin. Solid State Mater. Sci. **15**, 188 (2011).
[33]T. Kent, K. Tang, V. Chobpattana, M. A. Negara, M. Edmonds, W. Mitchell, B. Sahu, R. Galatage, R. Droopad, P. McIntyre, and A. C. Kummel, J. Chem. Phys. **143**, 164711 (2015).

[34]W. Wang, K. Xiong, R. M. Wallace, and K. Cho, J. Phys. Chem. C **114**, 22610 (2010).
[35]L. Lin and J. Robertson, Appl. Phys. Lett. **98**, 082903 (2011).
[36]V. Chobpattana, T. E. Mates, W. J. Mitchell, J. Y. Zhang, and S. Stemmer, J. Appl. Phys. **114**, 154108 (2013).
[37]X. Qin, B. Brennan, H. Dong, J. Kim, C. L. Hinkle, and R. M. Wallace, J. Appl. Phys. **113**, 244102 (2013).
[38]H. Dong, K. C. Santosh, X. Qin, B. Brennan, S. McDonnell, D. Zhernokletov, C. L. Hinkle, J. Kim, K. Cho, and R. M. Wallace, J. Appl. Phys. **114**, 154105 (2013).
[39]H. Dong, B. Brennan, X. Qin, D. M. Zhernokletov, C. L. Hinkle, J. Kim, and R. M. Wallace, Appl. Phys. Lett. **103**, 121604 (2013).
[40]D. M. Zhernokletov, P. Laukkanen, H. Dong, R. V. Galatage, B. Brennan, M. Yakimov, V. Tokranov, J. Kim, S. Oktyabrsky, and R. M. Wallace, Appl. Phys. Lett. **102**, 211601 (2013).
[41]R. Engel-Herbert, Y. Hwang, and S. Stemmer, J. Appl. Phys. **108**, 124101 (2010).
[42]Y. Yuan, L. Wang, B. Yu, B. Shin, J. Ahn, P. C. McIntyre, P. M. Asbeck, M. J. W. Rodwell, and Y. Taur, IEEE Electron Device Lett. **32**, 485 (2011).
[43]T. D. Lin, Y. H. Chang, C. A. Lin, M. L. Huang, W. C. Lee, J. Kwo, and M. Hong, Appl. Phys. Lett. **100**, 172110 (2012).
[44]R. Suzuki, N. Taoka, M. Yokoyama, S.-H. Kim, T. Hoshii, T. Maeda, T. Yasuda, O. Ichikawa, N. Fukuhara, M. Hata, M. Takenaka, and S. Takagi, J. Appl. Phys. **112**, 084103 (2012).